ARTICLE

Effect of Catalyst Properties on Hydrocracking of Pyrolytic Lignin to Liquid Fuel in Supercritical Ethanol

Qian Yao[a†], Zhe Tang[b†], Jian-hua Guo[a], Ying Zhang[a*], Qing-xiang Guo[a]

a. Collaborative Innovation Center of Chemistry for Energy Materials, Anhui Province Key Laboratory of Biomass Clean Energy and Department of Chemistry, University of Science and Technology of China, Hefei 230026, China

b. School of Chemical and Biological Engineering, Yancheng Institute of Technology, Yancheng 224051, China

(Dated: Received on September 30, 2014; Accepted on January 29, 2015)

The metal-acid bifunctional catalysts have been used for bio-oil upgrading and pyrolytic lignin hydrocracking. In this work, the effects of the metal-acid bifunctional catalyst properties, including acidity, pore size and supported metal on hydrocracking of pyrolytic lignin in supercritical ethanol and hydrogen were investigated at 260 °C. A series of catalysts were prepared and characterized by BET, XRD, and NH_3-TPD techniques. The results showed that enhancing the acidity of the catalyst without metal can promote pyrolytic lignin polymerization to form more solid and condensation to produce more water. The pore size of microporous catalyst was smaller than mesoporous catalyst. Together with strong acidity, it caused pyrolytic lignin further hydrocrack to numerous gas. Introducing Ru into acidic catalysts promoted pyrolytic lignin hydrocracking and inhibited the polymerization and condensation, which caused the yield of pyrolytic lignin liquefaction product to increase significantly. Therefore, bifunctional catalyst with high hydrocracking activity metal Ru supported on materials with acidic sites and mesopores was imperative to get satisfactory results for the conversion of pyrolytic lignin to liquid products under supercritical conditions and hydrogen atmosphere.

Key words: Pyrolytic lignin, Hydrocracking, Bifunctional catalyst

I. INTRODUCTION

As fossil fuels depletion and environmental issues deteriorated, the exploration of renewable and environment friendly energy resources has attracted considerable attention [1, 2]. Biomass is the most abundant green carbon source and therefore has been identified as scalable, economically viable, and potential carbon neutral feed stock for the production of fuels and chemicals via appropriate techniques. Among these techniques, fast pyrolysis is the most energy efficient and economically feasible way for biomass utilization, and has attracted a large number of researches over the past two decades [3−5]. The primary liquid product of this technique is generally known as bio-oil, which is composed of a large variety of organic compounds, mainly including acids, alcohols, aldehydes, ketones, esters, sugars, phenols, phenols derivatives, and a large proportion (13.5wt%−27.7wt%) of lignin-derived oligomers [6, 7]. The lignin-derived oligomers are also known as pyrolytic lignin (PL). Generally, the crude bio-oil is characterized by low vapor pressure, low heating value, high acidity, high viscosity, and high reactivity [1, 4, 8]. These poor properties of bio-oil significantly limit its direct utilization in current industrial systems. To improve the quality of bio-oil, researchers developed several techniques including hydrodeoxygenation [9], esterification [10], ketonization [11, 12], catalytic cracking [13], and steam reforming [14, 15].

A method to upgrade bio-oils in supercritical alcohols has drawn significant attention. The advantages of supercritical reaction media include faster mass and heat transfer, liquid-like density and dissolving power, and gas-like diffusivity and viscosity [16, 17]. Peng *et al.* upgraded pyrolysis bio-oil from rice husk in supercritical ethanol under a nitrogen atmosphere with aluminum silicate catalyst and in subcritical and supercritical ethanol using HZSM-5 as catalyst [18, 19]. Li *et al.* compared low-boiling fraction of bio-oil upgrade with different catalysts, $Pt/Al_2(SiO_3)_3$, Pt/C, and Pt/MgO, while the high-boiling fraction of bio-oil was upgraded over a series of supported monometallic and bimetallic catalysts under the supercritical methanol condition and hydrogen atmosphere [20, 21]. Tang *et al.* studied one step reaction of bio-oil upgrad-

†These authors contributed equally to this work.
*Author to whom correspondence should be addressed. E-mail: zhzhying@ustc.edu.cn

ing through hydrotreatment, esterification, and cracking in supercritical ethanol under hydrogen atmosphere using $Pd/SO_4^{2-}/ZrO_2$ /SBA-15 catalyst [22]. Dang *et al.* investigated the influence of experimental parameters like initial hydrogen, the mass ratio of solvent to bio-oil and reaction temperature on bio-oil upgrading process [23]. As we have previously shown, bio-oil can be separated effectively into two fractions: a complex mixture of organic compounds and PLs [6, 7]. PLs have pernicious effects on bio-oil properties such as high viscosity, high reactivity and low stability. Its upgrading is the most difficult in all the compounds in bio-oil. However, PLs contribute a lot to the high heating values of bio-oils due to their low oxygen content. In comparison with the broad investigation on the bio-oil upgrading in supercritical alcohols, much less attention has been paid to converting PLs to stable liquid compounds. Ford group [24, 25] explored single-step disassembly of lignin into monomeric cyclohexyl derivatives using a Cu-doped porous metal oxide as the catalyst in supercritical methanol at 300 °C without addition hydrogen. In their follow-up study [26], the same catalyst was used to convert an organosolv lignin into mixtures of aromatic products via hydrogen transfer at lower temperature (140−220 °C) in the presence of hydrogen and supercritical methanol. Tang *et al.* developed effective catalysts $Ru/ZrO_2/SBA$-15 and $Ru/SO_4^{2-}/ZrO_2/SBA$-15 to catalytic hydrocrack PL to liquid fuel in supercritical ethanol [27]. Huang *et al.* reported a Cu-doped MgAl mixed oxide catalyst was used to convert soda lignin to aromatics in single step without char formation in supercritical ethanol [28].

Usual properties of the catalysts including the acidity, pore size and supporting metal significantly influence the PL conversion, in this study, a series of catalysts with different acidity, pore size and supporting metal were designed and synthesized. The chemical and structural properties of these catalysts were characterized by BET, XRD and NH_3-TPD techniques. The catalytic activities of the catalysts were tested in the catalytic hydrocracking of PL in supercritical ethanol under hydrogen atmosphere.

II. EXPERIMENTS

A. Materials

PL in this work was obtained from the bio-oil that was produced through the fast pyrolysis of rice husk at about 550−600 °C [29]. PL precipitated was accomplished according to the method of Scholze and Meier [30, 31]. First, crude bio-oil was dropwise added into chilled deionized water under vigorous stirring. Then the dried precipitate was washed by ethyl acetate to remove some contamination such as fatty acid, long-chain alkanes, and other monomers. Finally, the PL was acquired by drying carefully under vacuum at 40 °C. Based on the elemental analysis data of an elemental analyzer (VARIO EL III, Elementar, Germany), the PL consisted of 60.21%C, 6.42%H, 2.07%N, and 31.30%O.

Ru(III) chloride hydrate (99.9%) was purchased from Strem Chemicals. Triblock copolymer $EO_{20}PO_{70}EO_{20}$ (P_{123}) and catalyst support (HY and HZSM-5) were purchased from Aldrich. Other reagents were purchased from Sinopharm Chemical Reagent Co., Ltd. All chemicals were used as received without further purification.

B. Catalyst preparation

SBA-15 was prepared according to the method described in Ref.[32]. ZrO_2/SBA-15 (designated as $Zr(X)$) and $SO_4^{2-}/ZrO_2/SBA$-15 (designated as $SZr(X)$) catalysts were synthesized via two step wetness impregnation, where X was the mass loading of ZrO_2 in catalyst and equals to 35wt% or 50wt% respectively. The detailed process can be seen in Ref.[27].

To prepare 3wt% supported Ru catalysts, 0.135 g Ru(III) chloride hydrate was impregnated in 2.0 g of $Zr(X)$, $SZr(X)$, HY, and HZSM-5, respectively. $Ru/ZrO_2/SBA$-15 (designated as $RuZr(X)$), $Ru/SO_4^{2-}/ZrO_2/SBA$-15 (designated as $RuSZr(X)$), RuHY, and RuHZSM-5 catalysts were prepared through the dry impregnation method. The solid products were calcined at 300 °C in a hydrogen and nitrogen atmosphere for 3 h at a heating rate of 1.0 °C/min to obtain the ultimate catalysts. The flow rates of hydrogen and nitrogen were 10 and 100 mL/min, respectively. $3wt\%Pd/ZrO_2/SBA$-15 (designated as PdZr(50)) was also synthesized via the same method as preparation of Ru-supporting catalysts.

C. Characterization of catalysts

X-ray diffraction (XRD) analysis was performed on a Philips X'Pert PROS X-ray diffractometer, which employed CuKα radiation. The data were recorded over a 2θ range of 10°−70° for wide angle.

Nitrogen adsorption-desorption isotherms were acquired from a Micromeritics ASAP 2020 system at 77 K. The Brunauer-Emmett-Teller (BET) equation was employed to calculate the surface area in the relative pressures range between 0.0 and 0.2. The pore size distributions were calculated based on the adsorption and desorption branches of the isotherms using the thermodynamic-based Barrett-Joyner-Halenda (BJH) method. The total pore volume was derived from the adsorption and desorption branches of the nitrogen isotherms at the single point of relative pressure P/P_0=0.97.

NH_3-temperature programmed desorption (NH_3-TPD) measurements were carried out to determine the acid properties of catalyst. The catalysts were first treated at 500 °C under helium flow (ultrahigh purity,

DOI:10.1063/1674-0068/28/cjcp1409167

40 mL/min) for 2 h and then cooled to 90 °C. The adsorption of ammonia was carried out at 90 °C for 1 h. After the catalyst was purged with helium flow at 90 °C for 2 h, the catalyst was heated up to 700 °C at the rate of 8 °C/min. The desorbed ammonia was measured by a gas chromatograph (GC-SP6890, Shandong Lunan Ruihong Chemical Instrument Co. Ltd., Tengzhou China) with a thermal conductivity detector (TCD).

The chemical compositions of catalysts were measured by Perkin Elmer Analyst 800 atomic absorption spectrometer.

D. Experimental procedure

A series of PL hydrocracking experiments were carried out, and the typical experimental process was described as follows. About 3.0 g PL, 33.3 g ethanol and 1.5 g catalyst were filled into a 150 mL autoclave (NS-50-C276, Anhui Kemi Machinery Technology Co., Ltd., China). The reactor was flushed with nitrogen and then hydrogen several times to remove the residual air. About 2.0 MPa H_2 was injected into the autoclave at room temperature. The reactor was heated up to 260 °C with an electric heating system and the experiments were kept at this steady temperature for 8 h. The pressure of the reactor was held up at about 9.5 MPa at 260 °C. After cooling to room temperature, the pressure was recorded and then the gas was collected for further analysis by gas chromatography (GC). The autoclave was opened and the liquid product was obtained. After centrifugation, the liquid was weighed through an analytical balance. Each experiment was repeated more than once and all data in this work were the average results.

For convenience of description, the liquid product obtained from different catalyst was designated as catalyst-oil, such as Zr(X)-oil, SZr(X)-oil, RuZr(X)-oil, RuSZr(X)-oil, RuHY-oil, RuHZSM-oil, and NoCat-oil (no catalyst oil).

E. Characterization of products

The organic components of the liquid product were analyzed by GC-MS (Thermo Trace DSQ (I)) with a TR-5MS fused-silica capillary column (30 m×0.25 mm i.d., 0.25 μm film thickness). The ethanol and ether content were analyzed by GC (GC1690, Kexiao, China) using n-propanol as an internal standard. The water content in the liquid samples was determined by Karl Fischer titration. The gas was collected by a gasbag and sampled for analysis using a GC (GC1690, Kexiao, China) with thermal conductivity detector (TCD) using an external standard method. The calibration gas mixture including H_2, CO, CO_2, CH_4, C_2H_4, C_2H_6, C_3H_6, and C_3H_8, obtained from Nanjing Specialty Gas was used to identify gas products distribution.

The calculation method of solid and liquid yield is the products weight divided by the initial weight of ethanol (33.3 g) and PL (3 g). The yield of gaseous products was measured by means of percentage difference. It was noticeable that the liquid products should include the organic compounds converted from PL, the water produced from PL, ethanol and the unreacted ethanol. Instead of the yield of liquid, the yield of organic compounds converted from PL (designated $Y_{\rm oil}$) could represent the catalytic effect on PL liquefaction. $Y_{\rm oil}$ was calculated according to the following equation.

$$Y_{\rm oil} = \frac{\text{Product weight (liquid, ethanol, water)}}{\text{Weight of initial PL}} \times 100\%$$

The real yield of organic compounds converted from PL could be slightly lower than that of $Y_{\rm oil}$, since a small amount of ethanol might react with the initial PL and produce organic products.

III. RESULTS AND DISCUSSION

A. Catalyst characterization results

The high-angle XRD patterns of SBA-15, Zr(X), SZr(X), RuZr(X), and RuSZr(X) (X=30, 50) samples are presented in Fig.1. It can be seen there were four new diffraction peaks at 2θ=30.2°, 35.2°, 50.3°, and 59.8° in Zr(X) diffraction curve compared with that of SBA-15, indexed as the (101), (110), (200), and (211) reflections of the tetragonal ZrO_2 phase, respectively. XRD diffraction peaks of SZr(X), RuZr(X), and RuSZr(X) were almost the same as those of Zr(X). The result showed that the introduction of $SO_4{}^{2-}$ and metal Ru into catalyst kept the characteristic peaks of ZrO_2 unchanged. In addition, the crystallite size of ZrO_2 particles was about 8.13 nm×4.33 nm according to the Scherrer formula. There were no other peaks in the high-angle region of RuZr(X) and RuSZr(X), indicating that Ru particles were highly dispersed on the prepared catalyst.

The BET surface area (BSA), micropore area (MA), average pore volume (APV), average pore size (APS), and chemical composition of SBA-15, Zr(X), SZr(X), RuZr(X), and RuSZr(X) (X=30, 50) catalysts are summarized in Table I. These texture parameters were acquired from nitrogen adsorption and atomic absorption measurements. The BSA, MA, APV decreased evidently after loading Ru and ZrO_2 on SBA-15 while the APS was slightly reduced. It implied the incorporation of Ru and ZrO_2 occupied the surface and inside pore channels of SBA-15 and the properties of the catalyst were changed. The assumption was confirmed by the following phenomenon, the BSA, MA, APV, and APS of the catalysts decreased gradually with the increasing ZrO_2 loading. However, the condition was a little different after treating support using sulfur acid, which

DOI:10.1063/1674-0068/28/cjcp1409167

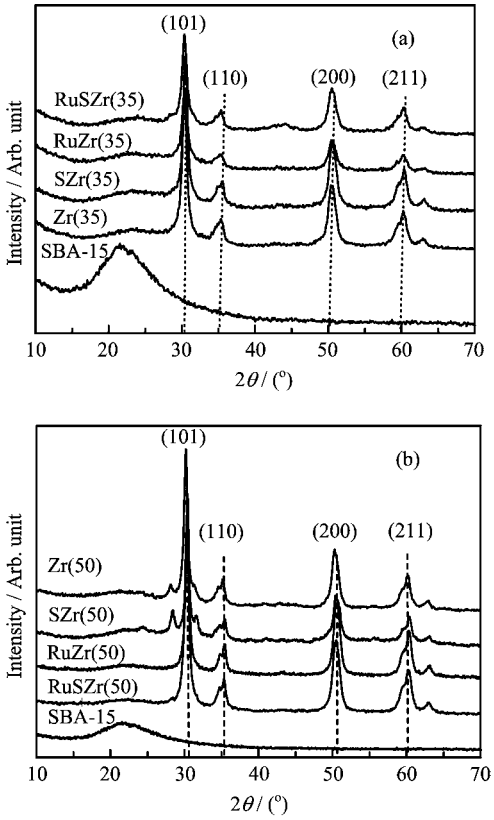

FIG. 1 XRD patterns of (a) Zr(35) series catalysts and (b) Zr(50) series catalysts.

TABLE I Textural properties and composition of catalyst. BSA and MA are in unit of m^2/g, APV in unit of cm^3/g, APS in unit of nm.

Sample	BSA	MA	APV	APS	Composition[a]
SBA-15	582.83	61.03	0.89	5.86	Pure silica
Zr(50)	200.47	30.85	0.22	4.85	Zr/Si=0.37
RuZr(50)	161.29	29.68	0.20	5.72	Zr/Si=0.38
SZr(50)	202.80	26.51	0.26	5.06	Zr/Si=0.37
RuSZr(50)	162.57	26.34	0.20	5.42	Zr/Si=0.38
Zr(35)	457.91	55.84	0.60	5.36	Zr/Si=0.23
RuZr(35)	402.31	36.40	0.55	5.51	Zr/Si=0.24
SZr(35)	460.92	53.26	0.62	5.46	Zr/Si=0.22
RuSZr(35)	402.37	32.91	0.54	5.50	Zr/Si=0.23

[a] The molar ratios of Zr to Si were obtained from the atomic absorption analysis.

can slightly enlarge the pore structure of their support, such as Zr(50) and SZr(50).

The NH_3-TPD measurement was performed to measure the acid density and acidity of the catalysts. The NH_3-TPD patterns of the catalysts including SZr(50), Zr(50), SZr(35), Zr(35), and SBA-15 are shown in Fig.2. The neutral SBA-15 showed no desorption peak, indicating that there was no acidity on the SBA-15. Except SBA-15, all the samples produced one NH_3 desorption peak at the range of 100−200 °C, which was corresponding to the weak acid. The peak area of the weak acid increased progressively with ZrO_2 content increasing from 35wt% to 50wt%. The result indicated the weak acid content of catalyst increased with the ZrO_2 loading augment. Moreover, it was found that the strong acid peak originated from sulfuric acid treatment. As presented in Fig.2, the peak corresponding to the strong acid sites was shifted to high temperature in the case of the SZr(50) sample compared with that of the SZr(35) sample. The observation indicated the higher ZrO_2 content of the SZr(X) led to the stronger and stable acid sites.

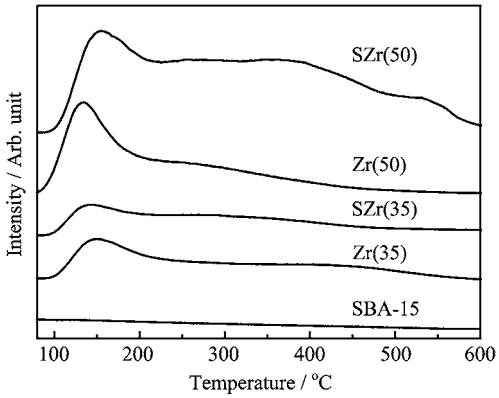

FIG. 2 NH_3-TPD curves of SZr(50), Zr(50), SZr(35), Zr(35), and SBA-15 catalysts.

B. Effect of catalytic acidity

Four kinds of catalyst supports and their Ru-supporting catalyst were designed to investigate the effect of catalytic acidity on PL liquefaction, the results are presented in Table II. It can be seen that liquid was the dominant product for each process. Without catalyst, PL was only partially hydrocracked in supercritical ethanol. In the presence of catalysts, more gas were obtained after reaction. This indicated that the catalysts could improve the cracking reaction of PL. In comparison with NoCat-oil, the application of SZr(50) caused Y_{oil} to sharply decrease. Meanwhile, this process produced more solid and water. Moreover, It was found that both Zr(50) and SZr(50) produced more solid and water and less PL liquefaction product than that of Zr(35) and SZr(35), respectively. SZr(X) produced more solid and water and less PL liquefaction product than that of Zr(X). From the result of NH_3-TPD test, we knew that the amount of acid would grow with the loading of ZrO_2 increase or treatment with sulfuric acid. All the results demonstrated the acid of catalysts would promote the PL polymerization and condensation but decrease the activity of the catalyst for PL liquefaction. The degree of polymerization and con-

DOI:10.1063/1674-0068/28/cjcp1409167

TABLE II The effect of catalytic acidity on PL liquefaction.

Catalysts	Y_{liquid}/wt%	Y_{solid}/wt%	Y_{gas}/wt%	Y_{oil}/wt%	Ethanol/wt%	Water/wt%
NoCat	88.96	4.27	6.77	51.28	90.46	4.74
Zr(35)	97.37	2.81	9.81	75.40	89.59	3.34
Zr(50)	88.17	4.59	7.23	56.18	91.26	4.36
SZr(35)	85.24	3.70	11.05	63.66	90.25	3.58
SZr(50)	86.17	5.12	7.90	36.73	89.22	7.28
RuZr(35)	88.72	2.05	9.22	81.68	89.25	3.24
RuZr(50)	86.91	0.30	12.79	99.51	86.46	3.83
RuSZr(35)	89.34	1.11	9.54	87.84	87.25	5.35
RuSZr(50)	88.98	0.93	10.09	96.10	84.73	6.33

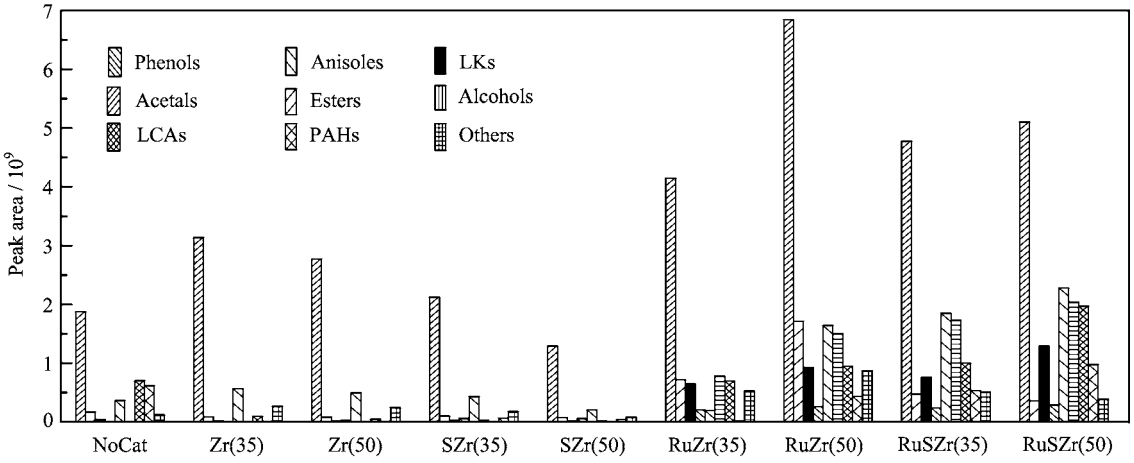

FIG. 3 Effect of catalytic acidity on the distribution of the liquid products. LKs: light ketones, LCAs: long-chain alkanes, PAHs: polycyclic aromatic hydrocarbons.

densation was increased with the amount and strength of acid increasing. Further incorporation of Ru on the support promoted gas production and limited the solid production. Meanwhile, Y_{oil} of these processes were significantly increased. The highest Y_{oil} was generated using RuZr(50). Y_{oil} of using RuSZr(50) was slightly lower than using RuZr(50). It was further indicated that higher acidity tended to promote PL polymerization to form more solid and condensation to produce more water.

In order to compare the product distribution in different oils, the hydrocracking products identified by GC-MS were classified into nine groups, which were phenols, anisoles, light ketones (LKs), acetals, esters, alcohols, long-chain alkanes (LCAs), polycylic aromatic hydrocarbons (PAHs) and others. During each experiment, the mass of the PL was the same, and the same sample injection amount was used for GC-MS analysis. Therefore, the corresponding chromatographic peak area of the compound on different chromatograms can be compared to reveal the change of its yields [33]. The product distribution with different acidity of catalyst is presented in Fig.3. The phenolic products were the dominant product. The peak area of phenols decreased more significantly using SZr(X) catalysts than Zr(X). The peak area of phenols increased significantly after Ru was introduced into the catalysts. Anisoles were also the decomposition products from the major structure of the PL [34]. With the increase of acidity of the catalysts, a slight increase of light volatile compounds such as LKs, acetals, esters, and alcohols was obtained after catalytic hydrocracking [35, 36], especially using Ru incorporated catalysts.

C. Effect of pore size

In porous materials, pore size affects the activity and selectivity of the catalysts in the reaction. In order to investigate the effect of pore size of the catalyst on PL liquefaction, the zeolites HY, HZSM-5 and their Ru-supporting catalyst were introduced into the system. The average pore size of Zr(50) (5.06 nm) is much larger than that of HY (0.55 nm), HZSM-5 (0.85 nm).

The NH_3-TPD patterns of the catalyst support including HY and HZSM-5 are shown in Fig.4. It is indicated that HY and HZSM-5 supports had the strong acidity sites, which were similar to Zr(50) support.

DOI:10.1063/1674-0068/28/cjcp1409167

TABLE III Properties of the liquid product under different pore size catalysts.

Catalysts	Y_{liquid}/wt%	Y_{solid}/wt%	Y_{gas}/wt%	Y_{oil}/wt%	Ethanol/wt%	Ether/wt%	Water/wt%
HZSM-5	74.77	5.57	19.66	17.85	28.43	40.78	40.78
HY	74.80	4.48	20.72	20.36	56.91	22.34	16.33
RuHZSM-5	83.18	2.75	14.07	30.30	77.28	7.52	12.14
RuHY	88.98	5.52	14.61	33.07	65.29	11.60	19.46
RuZr(50)	86.91	0.30	12.79	99.51	86.46	0.05	3.83

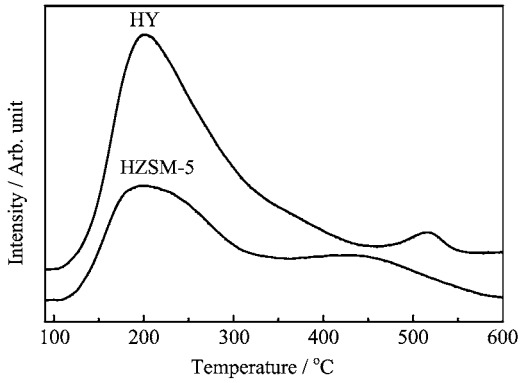

FIG. 4 NH_3-TPD curves of HY and HZSM-5 supports.

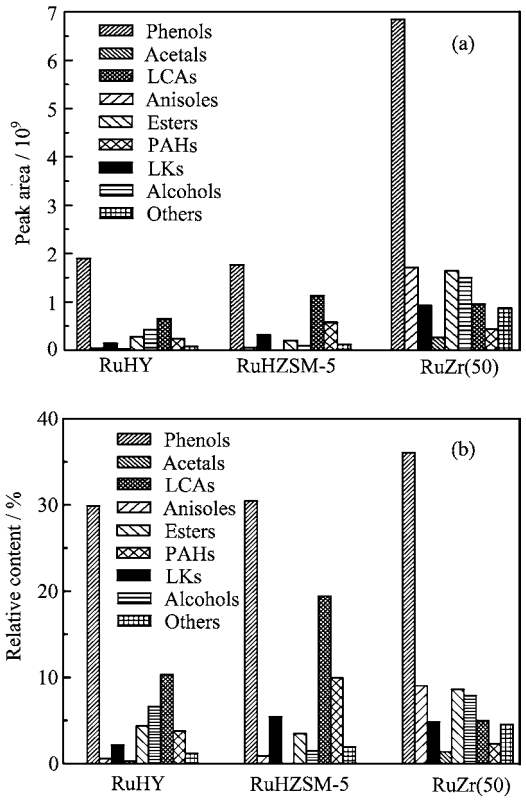

FIG. 5 Effect of pore size of catalysts on the distribution of the liquid products. (a) Based on the peak area, (b) based on the relative content.

From Table III, Y_{oil} of HY and HZSM-5 was only 20.36% and 17.85%, and their Y_{solid} was up to 4.48% and 5.57%, respectively. From the results of PL liquefaction under our developed system, it was known that incorporation of Ru on the supports would significantly decrease the effect of acidity on PL polymerization and condensation. Accordingly, further incorporation of Ru on the corresponding support could promote PL liquefaction. The Y_{oil} of RuHY and RuHZSM-5 were still much lower than that of RuZr(50). In addition, it can be found in Table III that significant amount of ethyl ether in RuHY-oil and RuHZSM-5-oil, which was trace in RuZr(50)-oil. HY and HZSM-5 support had much smaller pore size than Zr(50), which may result in the ether formation. The postulation was confirmed by the following facts. Firstly, the contents of ethanol in the two system were rather lower than that of RuZr(50), and secondly their water contents was much higher than that of RuZr(50). The consequences meant ethanol in the two systems reacted to form ether and water. As we know, the reaction was easy to process in acidic condition and microporous materials. These results indicated that pore size was another important factor on PL liquefaction.

The product distribution at different pore size of catalysts is presented in Fig.5. Figure 5(a) demonstrates that RuZr(50) catalyst can promote the PL cracking and produce much more liquid products than RuHY and RuHZSM-5 catalysts, which is consistent with Y_{oil}. Relatively, phenols were the dominant products by using all of these catalysts (Fig.5(b)). RuHY also tended to produce long-chain alkanes, alcohols, esters and PAHs. RuHZSM-5 tended to produce long-chain alkanes, PAHs, light ketones, and esters. The SBA-15 materials are synthesized in acidic media to produce highly ordered, two-dimensional hexagonal (space group p6mm) silica-block copolymer mesophases, and the pore sizes of SBA were in the range of 46−300 Å, besides, the pore volume fractions of SBA could be up to 0.85 [32]. HZSM-5 was consisted of two perpendicularly intersecting channels, and the pore size of HZSM-5 was only 5−6 Å. The pore structure of HY zeolite was 3-dimensional pore structure, and the pore size of HY was only 7.4 Å [37, 38]. Compared with the other two supporter, the pore size of the supporter RuZr(50) was much larger, and it produced more anisoles, esters and alcohols.

DOI:10.1063/1674-0068/28/cjcp1409167

TABLE IV The effect of supporting metal on PL liquefaction.

Catalysts	Y_{solid}/wt%	Y_{gas}/wt%	Y_{oil}/wt%	Ethanol/wt%	Ether/wt%	Water/wt%
PdZr(50)	1.61	16.12	81.26	86.36	0.031	5.33
RuZr(50)	0.30	12.79	99.51	86.46	0.051	3.83

D. Effect of the supporting metal of the catalyst

In order to understand the effect of the supporting metal on PL liquefaction, another common noble metal Pd was introduced in the system by using Zr(50) as support. Pd was chosen due to its strong hydrogenation capability. The results of these catalysts on PL liquefaction are given in Table IV. It can be observed that compared with Ru-supporting catalyst RuZr(50), Pd supporting catalyst PdZr(50) produced less gas and oil but more solid products. Therefore, compared with Pd, Ru-supporting catalyst was more suitable for hydrocracking PL to liquid compound and inhibiting polymerization and condensation, which could be due to the stronger hydrocracking activity of Ru.

IV. CONCLUSION

We investigated the effect of metal-acid bifunctional catalyst properties on PL liquefaction in supercritical ethanol and hydrogen atmosphere, including the acidity, pore size and supporting metal. It was noted that the acidity of support catalysts can promote PL hydrocracking. Meanwhile, the polymerization and condensation of PL would be increased with acidity increasing. Introducing Ru to acidic support would significantly suppress the effect of acidity on PL liquefaction. In Ru-supporting catalyst, appropriate pore size was also of great importance. Microporous catalyst support HZSM-5 and HY were apt to promote solid and gas production, which resulted from polymerization and condensation, and deep cracking of PL, respectively. The mesoporous catalyst supports developed in our lab, such as Zr(50) and SZr(50), were more suitable for PL liquefaction under hydrogen and supercritical ethanol. These catalysts effectively inhibited PL deep cracking, polymerization and condensation and increased the yield of liquid produced from PL. In addition, it was found that Ru possessed much better hydrocracking activity. It demonstrated that the acidic sites, mesopores supports and high hydrocracking activity of supported metal were in favor of PL liquefaction under supercritical condition in hydrogen atmosphere. The investigation on different catalysts and various supercritical reaction media is currently under processing to make it possible for the PL liquefaction in large scale.

V. ACKNOWLEDGMENTS

This work was supported by the National Basic Research Program of China (No.2012CB215306), the Program for Changjiang Scholars and Innovative Research Team in University of the Ministry of Education of China, and the Fundamental Research Funds for the Central Universities (No.WK2060190040).

[1] G. W. Huber, S. Iborra, and A. Corma, Chem. Rev. **106**, 4044 (2006).
[2] A. Corma, S. Iborra, and A. Velty, Chem. Rev. **107**, 2411 (2007).
[3] S. Czernik and A. V. Bridgwater, Energ. Fuel **18**, 590 (2004).
[4] R. P. Anex, A. Aden, F. K. R. P. Anex, A. Aden, F. K. Kazi, J. Fortman, R. M. Swanson, M. M. Wright, J. A. Satrio, R. C. Brown, D. E. Daugaard, A. Platon, G. Kothandaraman, D. D. Hsu, and A. Dutta, Fuel **89**, S29 (2010).
[5] C. J. Liu, H. M. Wang, A. M. Karim, J. M. Sun, and Y. Wang, Chem. Soc. Rev. **43**, 7594 (2014).
[6] B. Scholze, C. Hanser, and D. Meier, J. Anal. Appl. Pyrol. **58**, 387 (2001).
[7] R. Bayerbach, V. D. Nguyen, U. Schurr, and D. Meier, J. Anal. Appl. Pyrol. **77**, 95 (2006).
[8] D. Mohan, C. U. Pittman, and P. H. Steele, Energ. Fuel **20**, 848 (2006).
[9] E. Furimsky, Appl. Catal. A **199**, 147 (2000).
[10] Q. Zhang, J. Chang, T. Wang, and Y. Xu, Energ. Fuel **20**, 2717 (2006).
[11] C. A. Gartner, J. C. Serrano, D. J. Braden, and J. A. Dumesic, Chemsuschem **2**, 1121 (2009).
[12] L. Deng, Y. Fu, and Q. X. Guo, Energ. Fuel **23**, 564 (2009).
[13] S. Vitolo, M. Seggiani, P. Frediani, G. Ambrosini, and L. Politi, Fuel **78**, 1147 (1999).
[14] A. C. Basagiannis and X. E. Verykios, Catal. Today **127**, 256 (2007).
[15] C. Rioche, S. Kulkarni, F. C. Meunier, J. P. Breen, and R. Burch, Appl. Catal. B **61**, 130 (2005).
[16] A. Baiker, Chem. Rev. **99**, 453 (1999).
[17] D. Wen, H. Jiang, and K. Zhang, Prog. Nat. Sci. **19**, 273 (2009).
[18] J. Peng, P. Chen, H. Lou, and X. Zheng, Energ. Fuel **22**, 3489 (2008).
[19] J. Peng, P. Chen, H. Lou, and X. Zheng, Bioresource Technol. **100**, 3415 (2009).
[20] W. Li, C. Y. Pan, Q. J. Zhang, Z. Liu, J. Peng J, P. Chen, H. Lou, and X. M. Zheng, Bioresource Technol. **102**, 4884 (2011).
[21] W. Li, C. Y. Pan, L. Sheng, Z. Liu, P. Chen, H. Lou, and X. M. Zheng, Bioresource Technol. **102**, 9223 (2011).
[22] Z. Tang, Y. Zhang, Q. Lu, X. F. Zhu, and Q. X. Guo, Ind. Eng. Chem. Res. **48**, 6923 (2009).

DOI:10.1063/1674-0068/28/cjcp1409167

[23] Q. Dang, Z. Y. Luo, J. X. Zhang, J. Wang, W. Chen, and Y. Yang, Fuel **103**, 683 (2013).
[24] K. Barta, T. D. Matson, M. L. Fettig, S. L. Scott, A. V. Iretskii, and P. C. Ford, Green Chem. **12**, 1640 (2012).
[25] T. D. Matson, K. Barta, A. V. Iretskii, and P. C. Ford, J. Am. Chem. Soc. **133**, 14090 (2011).
[26] K. Barta, G. R. Warner, E. S. Beach, and P. T. Anastas, Green Chem. **16**, 191 (2014).
[27] Z. Tang, Y. Zhang, Q. Lu, and Q. X. Guo, Ind. Eng. Chem. Res. **49**, 2040 (2010).
[28] X. M. Huang, T. I. Koranyi, M. D. Boot, and E. J. M. Hensen, ChemSusChem **7**, 2276 (2014).
[29] Q. Lu, X. L. Yang, and X. F. Zhu, J. Anal. Appl. Pyrol. **82**, 191 (2008).
[30] B. Scholze, C. Hanser, and D. Meier, J. Anal. Appl. Pyrol. **58**, 387 (2001).
[31] B. Scholze and D. Meier, J. Anal. Appl. Pyrol. **60**, 41 (2001).
[32] D. Y. Zhao, J. L. Feng, Q. S. Huo, N. Melosh, G. H. Fredrickson, B. F. Chmelka, and G. D. Stucky, Science **279**, 548 (1998).
[33] X. J. Guo, S. R. Wang, Z. G. Guo, Q. Liu, Z. Y. Luo, and K. F. Cen, Appl. Energ. **87**, 2892 (2010).
[34] M. P. Pandey and C. S. Kim, Chem. Eng. Technol. **34**, 29 (2011).
[35] R. J. A. Gosselink, W. Teunissen, J. E. G. Dam, E. Jong, G. Gellerstedt, E. L. Scott, and J. P. M. Sanders, Bioresource Technol. **106**, 173 (2012).
[36] H. W. Park, J. K. Kim, U. G. Hong, Y. J. Lee, J. H. Song, and I. K. Song, Catal. Surv. Asia **17**, 119 (2013).
[37] A. Aho, N. Kumar, K. Eranen, T. Salmi, M. Hupa, and D. Y. Murzin, Fuel **87**, 249 (2008).
[38] S. R. Wang, Q. J. Cai, J. H. Chen, L. Zhang, X. Y. Wang, and C. J. Yu, Ind. Eng. Chem. Res. **53**, 13935 (2014).

DOI:10.1063/1674-0068/28/cjcp1409167